

## Use of Finite-Energy Sum Rules for a Numerical Study of Regge Behavior in a Unitarized $\pi$ - $\pi$ Veneziano Model\*

M. L. GRISS†

Physics Department, University of Illinois, Urbana, Illinois 61801

(Received 24 February 1970)

A simple single-channel  $K$ -matrix unitarization of the  $\pi$ - $\pi$  Veneziano model is performed. Inelastic effects corresponding to neglected channels are incorporated by giving the input, degenerate  $\rho$  and  $f^0$  trajectories an imaginary part above the  $4\pi$  inelastic threshold. Finite-energy sum rules are used to study the high- $s$  behavior for  $t < 0$ , and corrected trajectories are extracted. The input degeneracy is broken, with the  $\rho$  being shifted up to an intercept of about 0.6 as against the input 0.483. The importance of non-leading terms in the Regge expansion, through interference effects at intermediate energies, is noted. We examine the resulting deviation from crossing symmetry.

### I. INTRODUCTION

THE popularity of the Veneziano formula,<sup>1</sup> as a model for theoretical and phenomenological investigations, is well known.<sup>2</sup> The idea of having an expression for an amplitude that explicitly displays crossing symmetry and Regge asymptotic behavior is extremely desirable, but the most obvious defect of this model is its restriction to infinitesimally narrow resonances and corresponding lack of unitarity. Experimentally, resonances are narrow as compared with the average spacing between them, and it is claimed that the Veneziano model is a good zeroth approximation; however, most fits to the low-energy (resonance) region are forced to correct some, or all, of the widths and so incorporate unitarity.<sup>3</sup> The theoretical question of what happens to the Regge trajectories then arises.

This work studies the  $\rho$  and  $f^0$  trajectories and their residue functions in  $\pi$ - $\pi$  scattering within the framework of a unitarization of the Veneziano model. The  $\pi$ - $\pi$  system is simple kinematically, without the complications of spin, and has undergone many previous examinations<sup>4</sup>; it has been chosen here because of its well-studied singularity structure, and importance in any self-consistent dynamical scheme. The principal features in this calculation will be the unitarization of the model and the extraction of the resulting "corrected" trajectories and residue functions by use of the finite-energy sum rules (FESR).<sup>5</sup> The idea is to correct the low-energy resonance behavior, and to use the assumed duality to predict the high-energy asymptotic Regge behavior.

The present calculation is not to be considered as a complete dynamical scheme, but rather as the first of a series of iterative steps that will ensure both unitarity and crossing symmetry.<sup>6</sup> In this calculation we consider exact unitarity in the  $s$  channel to be more important than the deviation from crossing symmetry that will result.

It has become increasingly apparent that the effects of other channels must be included in calculations of this type.<sup>7,8</sup> Here we introduce an inelasticity to decouple the  $\pi$ - $\pi$  problem from the necessary full multichannel setup.

### II. OUTLINE OF METHOD

We ensure unitarity of the  $S$  matrix by expressing it in terms of a Hermitian  $K$  matrix,  $S_t = (1 + iK_t)/(1 - iK_t)$ . An arbitrary choice of  $K_t(s)$  ensures unitarity in one channel only, and in general it is difficult to get crossing symmetry as well. We will unitarize the  $s$  channel, and use the imaginary part so generated for physical  $s$  as input to FESR to determine  $t$ -channel Regge parameters. The FESR, as used here, need the scattering amplitude only for  $s \geq s_0$  (where  $s_0 = 4m_\pi^2$ , the elastic threshold), although unphysical  $t$  values may be required.

The Veneziano amplitude seems to describe experimental data quite well,<sup>3</sup> when one shifts the real-axis poles in  $s$  by some sort of "unitarization."<sup>9</sup> Since the required shifts are small, we have identified the  $K$  matrix with the Veneziano amplitude; the real-axis  $s$  poles are permitted in  $K$ . Of course, one must unitarize the correct  $s$ -channel isospin amplitudes.

We introduce  $s$ -channel partial waves of the familiar  $\pi$ - $\pi$  Veneziano functions  $V^I(s, t, u)$  by<sup>10</sup>

$$V^I_t(s) = \frac{1}{32\pi} \int_{-1}^1 d \cos \theta P_t(\cos \theta) V^I(s, t, u) \quad (2.1)$$

\* Work supported by the National Science Foundation under Grant Nos. NSF GP-13671 and NSF GP-8081.

† University of Illinois Fellow.

<sup>1</sup> G. Veneziano, *Nuovo Cimento* **57A**, 190 (1968).

<sup>2</sup> M. Jacob, lecture notes, Schladming, 1969 (unpublished); CERN Report No. TH-1010 (unpublished); in *Proceedings of the Lund Conference on Elementary Particles Lund, 1969*, edited by G. von Dardel (Berlinska, Lund, 1969); CERN Report No. TH-1052 (unpublished), and references therein.

<sup>3</sup> C. Lovelace, CERN Report No. TH-1041 (unpublished); F. Wagner, *Nuovo Cimento* **64A**, 189 (1969).

<sup>4</sup> G. F. Chew and S. Mandelstam, *Phys. Rev.* **119**, 467 (1960).

<sup>5</sup> R. Dolen, D. Horn, and C. Schmid, *Phys. Rev.* **166**, 1768 (1968).

<sup>6</sup> L. A. P. Balazs, *Phys. Letters* **29B**, 228 (1969).

<sup>7</sup> A. J. Dragt, *Phys. Rev.* **156**, 1588 (1967).

<sup>8</sup> A. W. Martin and R. W. Childers, *Phys. Rev.* **182**, 1762 (1969).

<sup>9</sup> F. Arbab, *Phys. Rev.* **183**, 1207 (1969).

<sup>10</sup> J. A. Shapiro, *Phys. Rev.* **179**, 1345 (1969).

and define an elastic  $K$ -matrix element by

$$K_I^I(s) = \rho(s) V_I^I(s),$$

where  $\rho(s)$  is the usual kinematic factor  $2q/\sqrt{s}$ . This leads to a  $T$ -matrix element

$$T_I^I(s) = \frac{S_I^I(s) - 1}{2i\rho(s)} = V_I^I(s) / [1 - i\rho(s) V_I^I(s)], \quad (2.2)$$

normalized to give

$$\frac{d\sigma^I}{dt} = \frac{1}{64q^2s\pi} |T^I(s, t, u)|^2.$$

Examining the  $T(s, t)$  obtained in this way, we find that the real-axis  $s$  poles which gave narrow infinite spikes, and obscured the Regge behavior, have been pushed onto the second sheet. These give bumps of finite height, obeying the unitarity bound. However, the widths decrease with increasing  $s$ , and appear to level off at small constant values,<sup>10</sup> again leaving isolated spikes. The Regge limit is still obscured.

As this point we make use of the FESR proposed by Dolen, Horn, and Schmid<sup>5</sup> as a means of smoothing out the bumps, and observing the Regge limit. These sum rules of the form

$$S_n^{I^I}(s_u, t) = \frac{1}{s_u^{n+1}} \int_{s_0}^{s_u} ds' s'^n \text{Im} T^{I^I}(s', t) \\ \cong \sum_i \beta_i(t) s_u^{\alpha_i(t)} / [\alpha_i(t) + n + 1] \quad (2.3)$$

relate the  $s$ -channel discontinuity  $\text{Im} T(s, t)$  to the  $t$ -channel Regge poles and residues. [ $\text{Im} T^{I^I}(s, t)$  is the  $t$ -channel isospin combination, evaluated in the  $s$ -channel physical region.]

The upper limit of integration should be within the region where the Regge expansion is valid; but if one accepts the idea of "duality," in which the local average of the low-energy amplitude (smoothing out the bumps) coincides with the extrapolation to low energy of the Regge expansion, it is found that  $s_u$  can be lower than one would initially expect.<sup>11</sup>

We can fix  $s_u$  around 5–12 GeV<sup>2</sup>; provided that  $n$  is not too large, we do get appreciable contributions to the integral from the lower few GeV<sup>2</sup>, and so we essentially determine the Regge parameters from the low- and intermediate-energy behavior.

We evaluate the sum rules  $S_n(s, t)$  for a range of  $s$  values and make a least-squares fit to determine the  $t$ -channel Regge parameters  $\alpha_i(t)$  and  $\beta_i(t)$ . Even with the advantage of the sum rule, we find the bumps are not sufficiently smoothed out to allow a satisfactory determination of the trajectories. Since this fit is per-

<sup>11</sup> This follows from the idea of "local duality," where local averaging is enough to display the Regge form. See Ref. 5 and C. Schmid, Phys. Rev. Letters 20, 689 (1968).

formed in a region of  $s_u$  values around 8 GeV<sup>2</sup>, or higher, it is clear that demanding only elastic unitarity of the amplitude is inadequate; in fact, inelastic effects have their onset with  $4\pi$  production at  $s = 16m^2 = 0.32$  GeV<sup>2</sup>,  $K\bar{K}$  production at  $s = 1$  GeV<sup>2</sup>, and  $N\bar{N}$  production at  $s = 4$  GeV<sup>2</sup>.

A full multichannel unitarization would be prohibitive. Since we are studying only the  $\pi\text{-}\pi$  system, it is more convenient to approximate the effect of other channels by the use of the "reduced"  $K$  matrix.<sup>12</sup> In the elastic region this is the usual  $K$  matrix, real and symmetric, but once inelastic thresholds are passed, it picks up an imaginary part which can easily be related to the inelasticity. In partial-wave form we let the (now inelastic)  $S$  matrix be

$$S_I^I(s) = \eta_I^I(s) e^{2i\delta_I^I(s)} \equiv e^{2i\Delta_I^I(s)}, \quad (2.4)$$

where  $\delta_I^I(s)$  is always real. One essentially defines  $K^I(s, t)$  by  $K_I^I(s) = \tan \Delta_I^I(s)$ , so that it becomes complex when  $\eta_I^I(s) < 1$  (in the inelastic region).

A natural and appealing way of introducing inelasticity into the "Veneziano-as- $K$ -matrix" model, is to give the input trajectories imaginary parts once inelastic thresholds are crossed. One expects the trajectories to be analytic functions of  $s$  with a right-hand cut only, beginning at the elastic threshold,  $s_0$ . The elastic cut is introduced by the  $K$ -matrix unitarization, so we give the trajectories an imaginary part from  $s = 0.32$  GeV<sup>2</sup>, the  $4\pi$  threshold. This procedure introduces extra parameters, which are determined by assuming a possible  $\rho$  elasticity  $X_\rho$  of 0.9–0.95.<sup>13</sup> For simplicity, we have chosen the functional form of the imaginary part to be linear. In the region around  $s_u$ , this is fairly indistinguishable from other possible considerations based on analytic trajectories and Regge behavior.<sup>14,15</sup>

### III. DETAILS OF CALCULATION

For the purposes of comparison it is convenient to consider simultaneously three types of calculation. These are

(i) the Veneziano model with complex trajectory functions<sup>16</sup> (referred to below as case CV), where an imaginary part is added to the trajectory function to correspond to the onset of the elastic cut;

(ii) the unitarized Veneziano model using the reduced  $K$  matrix to incorporate inelasticity (case RK);

<sup>12</sup> In particular, for the many-channel treatment, see G. E. Hite, Ph.D. thesis, University of Illinois, 1967 (unpublished).

<sup>13</sup> J. S. Ball and M. Parkinson, Phys. Rev. 162, 1504 (1968); 168, 1926 (1968); T. Brunila, M. Roos, and J. Pisut, CERN Report No. TH-972, 1969 (unpublished), for a more complete numerical evaluation.

<sup>14</sup> R. Z. Roskies, Phys. Rev. Letters 21, 1851 (1968); Yale Report No. 2726-543, 1969 (unpublished).

<sup>15</sup> B. R. Desai and P. Kaus, University of California, Riverside, Report No. UCR-34P107-83, 1969 (unpublished).

<sup>16</sup> M. L. Paciello, L. Sertorio, and B. Taglienti, Nuovo Cimento 63A, 1026 (1969).

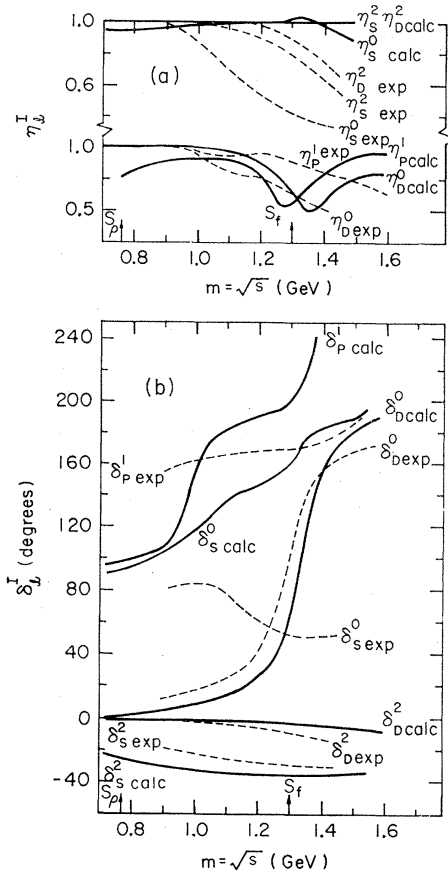


FIG. 1. Comparison of phase shifts  $\delta_I^l$  and inelasticities  $\eta_I^l$  calculated from the unitarized Veneziano model, RK (solid lines) with data in the  $\rho$ - $f^0$  region taken from Oh [Ref. 25 (dashed line)]. (a) Inelasticities. The bump  $\eta_s^0 > 1$  near  $s_\rho$  is the "ghost";  $\delta_s^0$  is also affected, rising instead of falling as the data do. (b) Phase shifts.

(iii) and the purely elastic  $K$ -matrix unitarization (case EK), which is a special instance of case RK, without any inelasticity.

We treat CV because it is the simplest numerically and is explicitly crossing symmetric; each of the trajectories  $\alpha(s)$ ,  $\alpha(t)$ , and  $\alpha(u)$  develops an imaginary part at the  $2\pi$  elastic threshold,  $x_0 = 4m_\pi^2 \simeq 0.08$  GeV<sup>2</sup>:

$$\alpha(x) = ax + b + i\theta(x - x_0)f_V(x). \quad (3.1)$$

The function  $f_V(x)$  should rise no more than linearly with  $x$ ,<sup>14,15</sup> although this is a statement on its asymptotic behavior, and does not preclude an involved low- $x$  structure.

The linear  $\text{Re}\alpha(s)$  given by Eq. (3.1) violates the, usual analytic form of the trajectory.<sup>17</sup> A curved  $\text{Re}\alpha(s)$  required by analyticity, is a basic problem in the use of the Veneziano model, as ancestors are introduced if

<sup>17</sup> P. D. B. Collins and E. J. Squires, *Regge Poles in Particle Physics* (Springer, Berlin, 1968), pp. 70-72.

$\alpha(t)$  is curved in the region where  $t < 0$ .<sup>18</sup> Actually it is necessary to have  $f_V(x)/x \rightarrow 0$  as  $x \rightarrow \infty$  so that the correct Regge limit (the signature factor)<sup>19</sup> is obtained, but in this calculation we require  $\alpha(s)$  only up to a finite value of  $s$ , no more than 15-20 GeV<sup>2</sup>, and so it is simplest just to use a linear form  $f_V(x) = C_V(x - x_0)$ .<sup>20</sup>

For the RK calculation, we perform the unitarization using the partial-wave decomposition of  $V^I(s, t)$ , and resum the corrected partial waves to obtain  $T^I(s, t)$ . In this case the input trajectory has the form

$$\alpha(x) = ax + b + i\theta(x - \bar{x}_1)f_K(x), \quad (3.2)$$

where the imaginary part now begins at the first inelastic threshold, the  $4\pi$ , with  $\bar{x}_1 = 16m_\pi^2 \simeq 0.32$  GeV<sup>2</sup>. This makes  $V^I(s, t)$  become the complex, "reduced"  $K$  matrix. The elastic imaginary part is put in by the unitarization. Again  $f_K(x)$  is linear,  $C_K(x - \bar{x}_1)$ . If  $C_K = 0$ , we get only the elastic part, and this is the purely elastically unitary EK.

The parameters of the trajectory,  $a$ ,  $b$  and  $C$ , and the over-all scale,  $g$ , of the amplitude  $V^I(s, t)$  are obtained from details of the low-energy  $\pi$ - $\pi$  system.

(i) The position of the  $s$ -channel resonances, at  $s_n$ , are given by  $\text{Re}\alpha(s_n) = as_n + b = n$ . We use the Lovelace<sup>21</sup> values,  $a = 0.885$  GeV<sup>-2</sup>,  $b = 0.483$ ,<sup>22</sup> obtained from the  $\rho$  at  $s_1$  and the Adler condition,  $\alpha(m_\pi^2) = \frac{1}{2}$ . (These are different from the values  $a = 1.015 \pm 0.17$  GeV<sup>-2</sup> and  $a = 0.406 \pm 0.12$ , obtained if one assumes that the  $\rho$  and  $f^0$  lie on a degenerate trajectory.<sup>23</sup>)

(ii) We relate the constant  $C_V$  to the  $\rho$  width  $\Gamma_\rho$  and fix  $g$  from the usual  $\rho\pi\pi$  coupling constant  $f_{\rho\pi\pi}$  ( $f^2/4\pi = 2.1-2.5$ ). Near the  $\rho$  pole,

$$V^I(s, t, u) = 16\pi g \frac{R_1(t) - R_1(u)}{a(s_1 - s) - i \text{Im}\alpha(s)} = 16\pi g \frac{t - u}{m_\rho^2 - s - i[\text{Im}\alpha(s)/a]}. \quad (3.3)$$

<sup>18</sup> The approach to the treatment of ancestors, which are unavoidable in the Veneziano model with analytic (hence curved) trajectories, is to show that the coupling of the ancestors can be considered negligible, as in Ref. 16.

<sup>19</sup> We ensure the correct signature factor by enforcing  $s$ - $u$  crossing symmetry in the FESR.

<sup>20</sup> In fact, even if  $\alpha(s)$  is analytic, with  $f(s)$  having an appropriate limiting behavior,  $\alpha(s)$  is usually considered to obey a doubly subtracted dispersion relation, and so the departure from linearity only displays itself at large  $s$  values. This point is stressed in an examination of baryon trajectories by R. M. Spector, *Phys. Rev.* **173**, 1761 (1968), where he finds an  $f(s) \simeq 0.135(s - 0.95)$ , to be compared with the value used in our CV of  $f(s) \simeq 0.167 \times (s - 0.08)$ . It is the smallness of  $f(s)$  that gives the decoupling of Ref. 18.

<sup>21</sup> C. Lovelace, *Phys. Letters* **28B**, 264 (1968).

<sup>22</sup> These values of  $a$  and  $b$  give rise to a "ghost" (pole with negative residue) at  $s_2$ , in  $l=0$ , below the  $f^0$ . A slight change in  $a$  and  $b$  could correct this (Ref. 10), but it does not affect our purpose, and, as seen in Fig. 2, the violation of unitarity is not large.

<sup>23</sup> The trajectories  $\alpha_\rho(s)$ ,  $\alpha_{f^0}(s)$  are necessarily degenerate in the original Veneziano model, because of the absence of "exotic" resonances in the  $I_3 = 2$  channel, and the constraints of crossing symmetry.

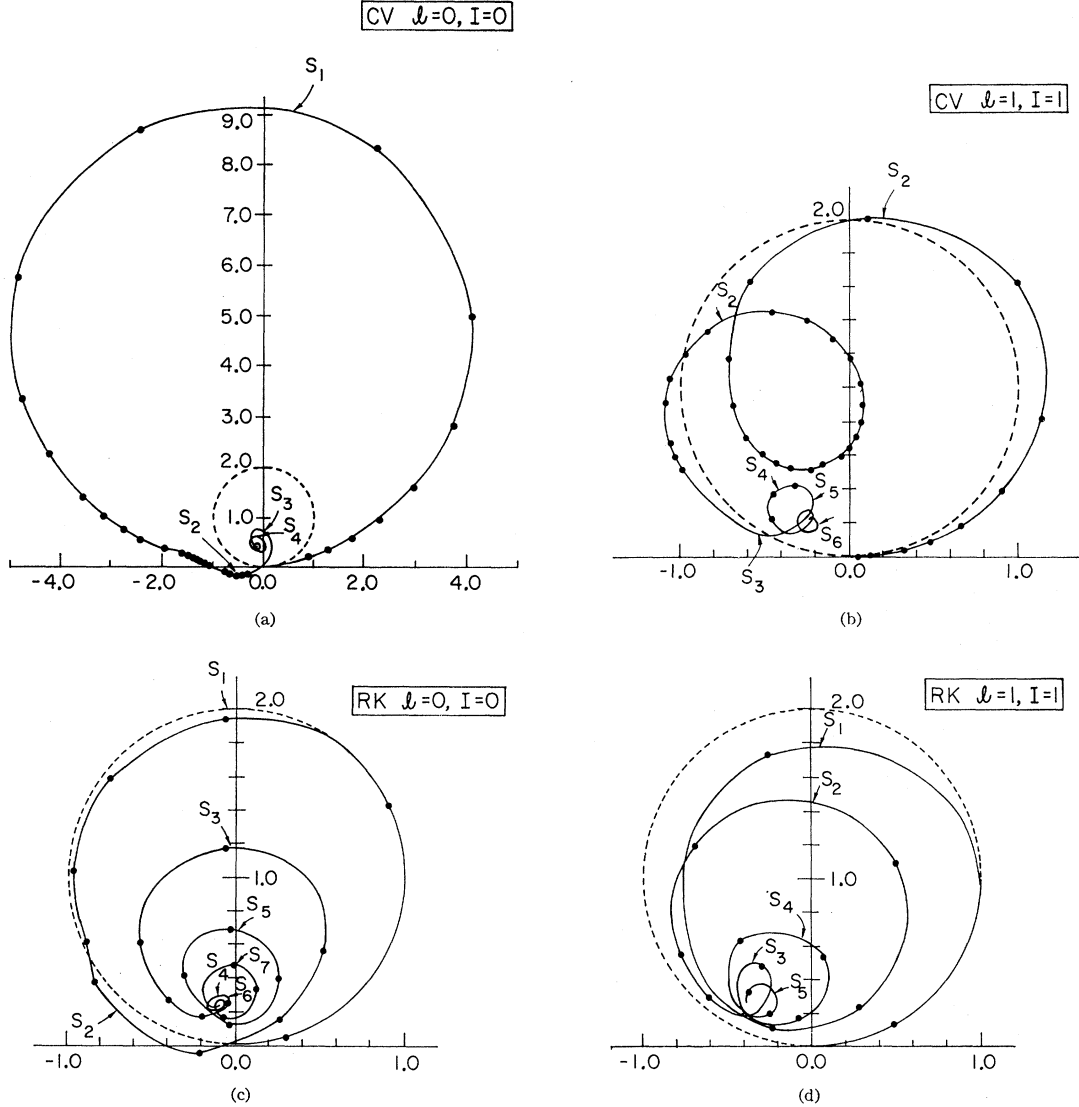


FIG. 2. Argand diagrams of the CV and RK partial-wave amplitudes  $a_l^I = 2\rho(s)T_l^I(s)$ . The dashed circle is the unitarity circle, of radius 1. The first few resonance positions  $s_n$  are marked with arrows. (a) Complex Veneziano  $l=0, I=0$ . Note that almost all the low-energy points fall outside of the unitarity circle. Note also the effect of the "ghost" at  $s_2$ . (b) Complex Veneziano,  $l=1, I=1$ . The dots on the solid line indicate increments in  $s$ ,  $\Delta s = 0.05 \text{ GeV}^2$ . (c) Unitarized Veneziano RK,  $l=0, I=0$ . Here only the "ghost" at  $s_2$  lies outside of the circle, and not by much. (d) Unitarized Veneziano,  $l=1, I=1$ . The dots now indicate increments of  $s$ ,  $\Delta s = 0.25 \text{ GeV}^2$ .

This corresponds to

$$T^l(s, t) = f_{\rho\pi\pi^2}(t-u)/(m_\rho^2 - s - im_\rho\Gamma_\rho). \quad (3.4)$$

So with  $\Gamma_\rho = 0.125 \text{ GeV}^2$  we get  $C_V = 0.167 \text{ GeV}^{-2}$  and  $g = 0.5-0.6$ .

(iii) For EK,  $\text{Im}\alpha(s) = 0$  ( $C_K = 0$ ) so that we have  $\Gamma_\rho m_\rho = \frac{1}{3}\rho(s_\rho)(2k_\rho)^2g$ , with  $(2k_\rho)^2 = s_\rho - 4m_\pi^2$ , which gives  $g = 0.614$ . This is the value of  $g$  used in all three cases for comparison.

(iv) When  $C_K \neq 0$ , corresponding to the inclusion of inelastic effects beginning at  $\bar{s}_1$ , we identify  $m_\rho\Gamma_\rho^{\text{el}} = \frac{1}{3}\rho(s_\rho)(2k_\rho)^2g$  as the elastic width and  $m_\rho\Gamma_\rho^{\text{in}} = \text{Im}\alpha(s_\rho)/a$  as the inelastic width. Choosing a total

width at the  $\rho$ ,  $\Gamma^{\text{tot}} = \Gamma_\rho^{\text{el}} + \Gamma_\rho^{\text{in}} \cong 0.135 \text{ GeV}^2$ , and an elastic width  $\Gamma^{\text{el}} \cong 0.120 \text{ GeV}^2$ , corresponding to a  $\rho$  elasticity  $X_\rho \cong 0.9$ , we fix  $C_K = 0.384 \text{ GeV}^{-2}$ .

This is an artifice to introduce an imaginary part to the trajectory to approximate the effects of inelasticity, and the exact low-energy behavior should not be taken too seriously.<sup>24</sup> However Fig. 1 does indicate some

<sup>24</sup> The  $\rho$  resonance is almost entirely elastic, although a multi-channel resonance fit by Ball and Parkinson (Ref. 13) indicates a possible elasticity  $X_\rho = 0.95$ . Use of this value in RK, above, gives a value of  $\eta$  much closer to 1 than do the data of Ref. 25. We prefer a smaller  $X_\rho \approx 0.9$ , which then gives  $X_\rho^0 \approx 0.8$ ; this is too small. [G. Ascoli *et al.*, Phys. Rev. Letters 21, (1969) find  $X_\rho \rightarrow 4\pi$  about 0.9,  $\Gamma_\rho^{\text{tot}} = 0.145 \text{ GeV}$ .] To fit actually the data of Ref. 25, we would have to abandon the simple linear form, Eq. (3.2).

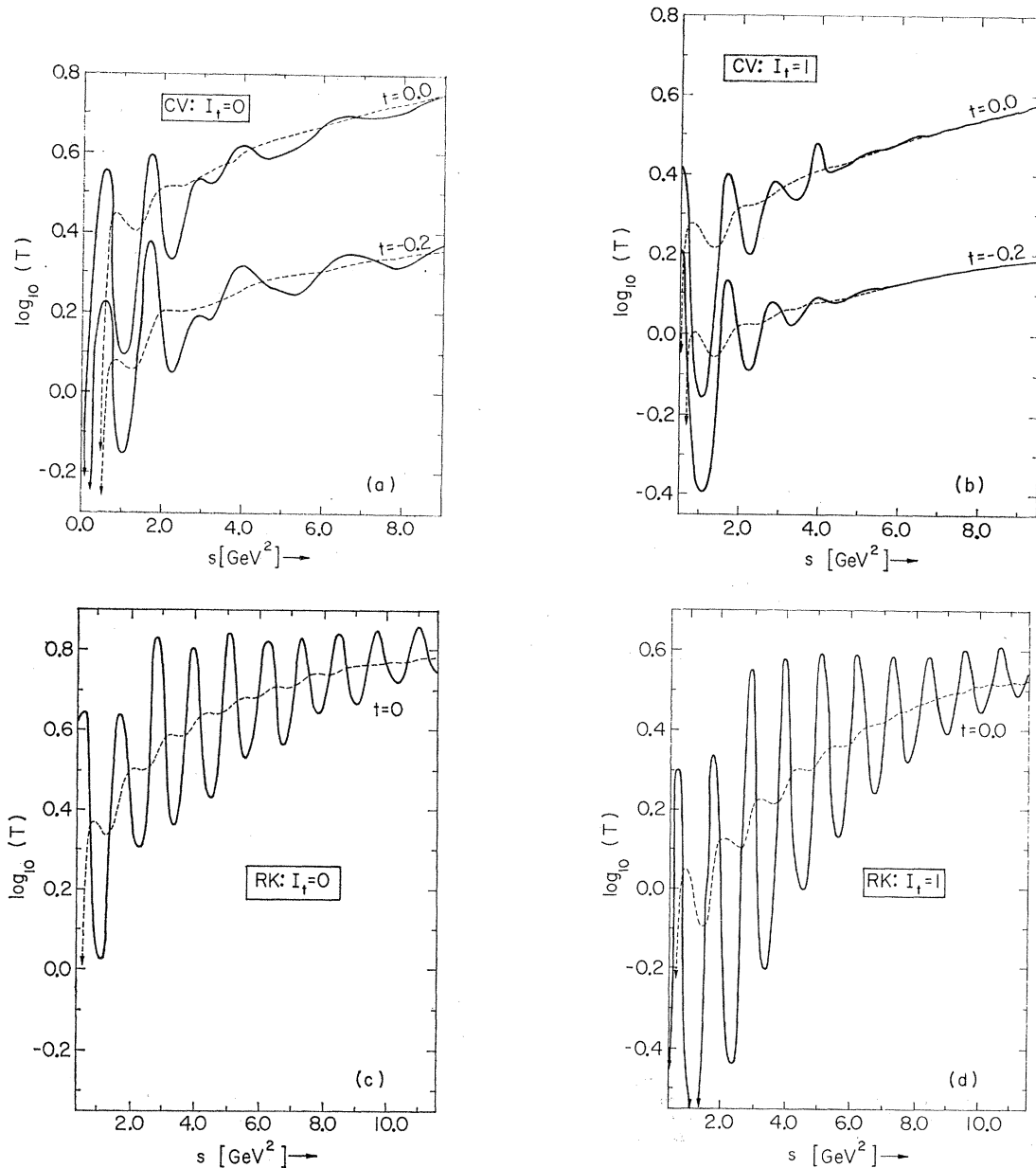


FIG. 3. Plots of  $\log_{10} \text{Im} T^{l_t}(s, t)$  (solid line) and corresponding FESR,  $\log_{10} S_0^{l_t}(s, t)$  (dashed line). The FESR has been multiplied by  $\alpha(t)+1$ , so that it is the average about which  $\text{Im} T^{l_t}$  clearly oscillates. The smoothing effect is obvious. (a)  $I_t=0$  ( $f^0$  exchange) for CV at  $t=0, -0.2 \text{ GeV}^2$ . (b)  $I_t=1$  ( $\rho$  exchange) for CV at  $t=0, -0.2 \text{ GeV}^2$ ; the Regge limit is attained sooner than in (a). (c)  $I_t=0$  ( $f^0$  exchange) for RK,  $t=0 \text{ GeV}^2$ . (d)  $I_t=1$  ( $\rho$  exchange) for RK,  $t=0 \text{ GeV}^2$ .

agreement with the data of Ref. 25, even for this simple linear form.

The behavior of some of the lower partial waves for the cases CV and RK can be seen in the Argand diagrams of Fig. 2. There are two features of principal interest. One is that even with the imaginary part

<sup>25</sup> B. Y. Oh *et al.*, Phys. Rev. Letters **23**, 331 (1969). Their study of  $\pi\pi$  scattering obtained from  $\pi^-p \rightarrow \pi^-\pi^+n$ ,  $\pi^-p \rightarrow \pi^-\pi^0p$  and  $\pi^-d \rightarrow \pi^-\pi^+pp$  covers our 1-2-GeV<sup>2</sup> region in  $s$ , and indicates quite considerable inelasticity in the  $S$ ,  $P$ , and  $D$  waves.

added in CV, the  $I=0$   $S$  wave, and to a lesser extent the  $I=1$   $P$  wave, greatly exceed the unitarity bound for  $s$  values extending beyond the  $f^0$  resonance. These are the waves that are principally affected by the unitarization in RK, and, apart from them, the complex Veneziano model CV is fairly unitary. (The  $l=2$  and  $l=3$  partial waves fall well within the unitary circle).

The other important feature is that for values of  $s$  above  $s_4 \approx 4.0 \text{ GeV}^2$ , the amplitudes  $a_i = 2\rho(s)T_i$  seem to be spiralling in towards a point near  $\text{Re} a_i \approx -0.2$ ,

$\text{Im}a_l \approx 0.25$ , with decreasing radii. The exact point is not fixed, and varies from example to example, as do the exact shapes of the loops. This behavior can be crudely understood in terms of a resonance of elasticity  $X(s)$  superimposed on a background  $B(s)$ , where both  $X$  and  $B$  vary slightly over the position of the resonance; if  $X$  and  $B$  are exactly constant, we expect a circle of radius  $X$  about the point  $B+iX$ . In fact, the Veneziano model CV gives a partial-wave amplitude of this form. In the neighborhood of the pole  $s_n$  that is resonating, the remaining poles in the infinite sum contribute to the "background"  $B$ , and presumably make up the Regge average that the full amplitude oscillates about in a duality sense. The interesting point is that the unitarized case RK displays essentially the same behavior, and so is likewise dual and presumably has Regge behavior. Purely elastic unitarization does not give this spiralling behavior.

Going over to the full amplitude, we see that only in the CV and RK cases do the resonance bumps smooth out, resulting in the awaited Regge asymptotic behavior, and this at a fairly high  $s$  value. The imaginary part of the amplitude,  $\text{Im}T^I(s,t)$ , is shown as the solid lines, in Fig. 3, and it is clear that pushing the poles off the real axis by increasing amounts does smooth out the resonance bumps. In EK only the elastic widths enter, and they decrease in the region examined, causing large narrow peaks.<sup>26</sup>

Use of the FESR is now made, in order to smooth out the bumps in a duality sense; if duality were not true, we would have to take the upper limit of the FESR as far as we would go to observe the Regge behavior directly in  $\text{Im}T(s,t)$ .<sup>27</sup> Some smoothing would result, but the bumps would still be seen. In Fig. 3 we plot as the dashed line the value  $[\alpha(t)+1]S_0(s,t)$ , superimposed on the amplitude to which it relates.

Except in the EK case, the Regge behavior of the FESR has set in by about 4 GeV<sup>2</sup> in CV and 8 GeV<sup>2</sup> in RK, a clear improvement. One must conclude that EK does not have smooth Regge behavior, and that duality does not hold for it, although there is some smoothing. In fact, the  $I_t=1$  EK amplitude oscillates violently through positive and negative values, and so does its FESR.

The FESR require the input  $\text{Im}T(s,t)$  at values of  $s$  and  $t$  that can lie outside of the  $s$ -channel physical region. This is a problem encountered in many dispersion-relation-type techniques; although  $s$  is restricted to run along the physical right-hand cut,  $s \geq s_0$ , for a fixed negative  $t$ , the lower  $s$  values correspond to

unphysical points and a continuation in  $t$  is required. In CV this continuation is provided by the explicitly continuable form of the gamma functions, while in RK,  $T(s,t)$  is represented by a Legendre series. The  $t$  values needed correspond to values of  $z_s = \cos\theta_s$ , greater than 1 in magnitude. Although at these values of  $s$ , the amplitudes  $T_l(s)$  are strongly decreasing as  $l$  increases, the Legendre functions  $P_l(z_s)$  behave as  $z^l$ , and cause the series to diverge; the attitude adopted here is to truncate the sum when the product  $T_l(s)P_l(z_s)$  reaches its smallest value.<sup>28</sup>

In the original Veneziano model CV, the nearest singularity which determines the Lehmann ellipse of convergence of the series is a  $t$  pole ( $z > 1$ ) or  $u$  pole ( $z < 1$ ) at  $\alpha(t_1)=1$  and  $\alpha(u_1)=1$ . With our choice of parameters,  $u_1=t_1 \approx 0.584$  GeV<sup>2</sup>. The trouble caused by  $u \geq u_1$  corresponds to  $s \leq 4m_\pi^2 - t - u_1 \approx -t - 0.504$  GeV<sup>2</sup>. Because the FESR are done for a fixed negative  $t$  in the range  $|t| \leq 0.8$  GeV<sup>2</sup>, this troublesome region is not an appreciable part of the region of integration ( $s_0 \leq s \leq 8-14$  GeV<sup>2</sup>).

In the unitary case one expects the nearest singularity to be the start of the  $u$  or  $t$  unitarity cuts, increasing the above "bad- $s$ " region to  $s < |t|$ . Our method does not unitarize the  $u$  or  $t$  channels and so we will still use the partial-wave series to continue to nonphysical values of  $t$ ,<sup>29</sup> as is done in the application of the FESR to experimental data.<sup>5</sup> We do not expect this region to contribute much to the FESR, and even restricting the integral to physical points only does not change the result much.

The FESR are calculated using a simple trapezoidal integral, with enough points to cover the resonance peaks smoothly. (About 200 points for  $s$  from 0.1 to 10 GeV<sup>2</sup>.) The Regge behavior of the FESR is quite clear by  $s$  about 5-9 GeV<sup>2</sup>.

We now extract effective trajectory and residue functions by making a simple least-squares fit to

$$\ln[S_n^I(N,t)] = A(t) \ln N + B(t), \quad (3.5)$$

with the behavior

$$S_n^I(N,t) \approx \beta_e(t) N^{\alpha_e(t)} / [\alpha_e(t) + n + 1],$$

giving

$$A(t) = \alpha_e(t), \quad B = \ln \frac{\beta_e(t)}{\alpha_e(t) + n + 1}. \quad (3.6)$$

If in this low- $s$  region we can identify the effective trajectory with the leading trajectory, we expect a behavior like that of the Veneziano model CV, with

$$\alpha_e(t) = at + b \quad \text{and} \quad \beta_e(t) = \tilde{\beta}^t a^{\alpha_e(t)} / \Gamma(\alpha_e(t)), \quad (3.7)$$

with  $\tilde{\beta}^t$  a constant.

<sup>28</sup> The partial-wave amplitudes are evaluated by numerical integration, using a 12- or 24-point Gaussian rule, so that very high  $l$  values, instead of giving  $T_l \approx 0$ , give large  $T_l$  because of numerical inaccuracies. We wish to truncate the sum before this point.

<sup>29</sup> The series for  $\text{Im}T(s,t)$  is, of course, supposed to converge in a larger ellipse, in the  $z$  plane, corresponding to the edge of the double spectral function as nearest singularity.

<sup>26</sup> This behavior for the widths is pointed out by Shapiro (Ref. 10), and in our case can be seen by using CV with  $\text{Im}\alpha(s) = \text{const}$ . The resulting amplitude is very similar to EK in over-all behavior.

<sup>27</sup> A point to be noted is that if we use a crude extrapolation procedure, say, that of using  $s^{\alpha(t)}$  in the low-energy region, instead of the possibly more correct  $P_{\alpha(t)}(z_t)$  or some other modified form [e.g., that suggested by L. Sertorio and L. L. Wang, Phys. Rev. 178, 2462 (1969)], we can expect the useful  $s_u$  to be somewhat higher.

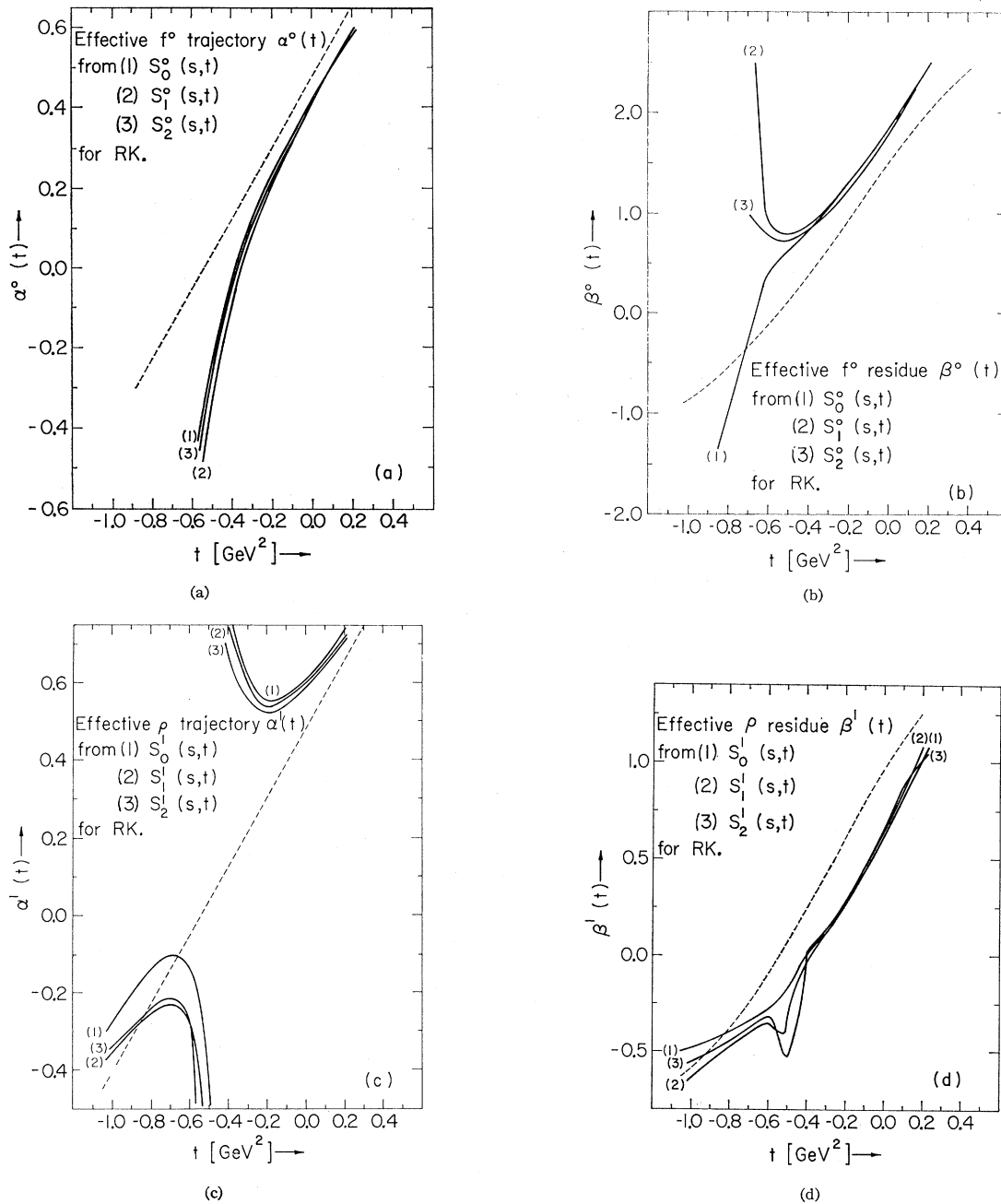


FIG. 4. Trajectories and residues calculated from  $S_n^{l,t}(s,t)$  in the unitarized Veneziano model RK. The dashed lines are the input trajectory  $\alpha_{in}(t) = 0.885t + 0.483$  and the leading residue  $\beta_0^{l,t}(t)$ . (a) Effective  $f^0$  trajectory  $\alpha^0(t)$  obtained by fit to (1)  $S_0^0(s,t)$ , (2)  $S_1^0(s,t)$ , and (3)  $S_2^0(s,t)$  with  $s$  in the range 9.5–13 GeV<sup>2</sup>; the mean error is  $\pm 1 \times 10^{-3}$ . (b) Corresponding residue  $\beta^0(t)$ . (c) Effective  $\rho$  trajectory  $\alpha^1(t)$  obtained by fit to (1)  $S_0^1(s,t)$ , (2)  $S_1^1(s,t)$ , and (3)  $S_2^1(s,t)$ , with  $s$  in the range 9.5–13 GeV<sup>2</sup>. The mean error is  $\pm 1 \times 10^{-3}$ . (d) Corresponding residue  $\beta^1(t)$ .

For small values of  $t$  down to  $-0.1$  GeV<sup>2</sup>, the fits are fairly good, improving if  $N$  is large, and  $\alpha_e(t)$  and  $\beta_e(t)$  do not deviate much from the input  $\alpha(s)$  and  $\beta(s)$ . The close agreement between  $\text{Im}T(N,t)$  and  $S_n(N,t)$  in the CV case, shows the validity of the FESR as used in this manner. But as  $t$  approaches and passes  $-0.4$  GeV<sup>2</sup>, strange-looking dips and peaks (Figs. 4) are obtained.

These dips are far more severe in the RK case than in CV, and change with different moments  $n$  in  $S_n(s,t)$ . In order not to overemphasize the higher  $s$  values in the FESR,  $n$  not larger than 2 was used. The shifting of these peaks [occurring near  $\beta(t) = 0$ ;  $t \approx -0.55$  GeV<sup>2</sup>] with the different moments  $n$ , leads one to consider the possibility that they are due to the interference of the

leading trajectory with the daughters. In the case CV, the first daughter trajectory and residue is displayed in Fig. 5. The daughter residue is small and goes through zero at the same time as the leading residue, but because the behavior is different can lead to an interference effect. At the  $s$  values used, the imaginary part added has not caused the oscillations of the poles to die completely away, and this probably enhances the effect of the interference. At larger values of  $N$ , up to 20 GeV<sup>2</sup>, we get a strictly one-trajectory fit without the interference.

The more prominent interference effects in the RK case can be traced to the fact that in the unitarization, the  $I_s=2$  amplitude is purely elastic, and obtains a large imaginary part, which behaves as  $0.3s^{\alpha^2(t)}$  with  $\alpha^2(t) \cong 0.435t - 0.01$ . In the case CV, the amplitude for  $I_s=2$  is proportional to  $F(u,t)$  (see the Appendix) which has no direct-channel resonances, and so has no imaginary part.

We also tried fitting with two trajectories. Although the peaks now obtained in the leading trajectory were less significant, and a fairly large "effective daughter" was indicated, the method is not accurate enough to separate the trajectories reliably. This casts doubt on its use on data, with inherently lower accuracy. Nevertheless, it must be concluded that the inclusion of secondary terms in the expansion for values of  $s$  around 7–10 GeV<sup>2</sup> is important.

Using a linear fit to the output trajectories, one sees that the input is followed fairly closely, but that the output  $\rho$  trajectory lies somewhat above the input, with  $\alpha_\rho(0) \cong 0.6$ , while the output  $f^0$  seems to fall below the input, with  $\alpha_f(0) \cong 0.43$ . Thus the exchange degeneracy is broken by the unitarization. This output  $\rho$  intercept agrees with the commonly found value of about 0.57, when fitting high-energy data, although the resonances on the  $\rho$  trajectory dictate a value certainly less than 0.483, as seen just after Eq. (3.2).

Because of the impossibility of using the partial-wave series to continue the unitarized amplitude to  $t > 0.08$  GeV<sup>2</sup>, and the limited accuracy that manifested itself above, no attempt was made to alter the input parameters to obtain the closest self-consistency; to do so would require a form for input of nondegenerate trajectories.<sup>30</sup> Possible corrections for the above difficulties are discussed in Sec. IV.

#### IV. CONCLUSIONS AND DISCUSSION

The major conclusions of this work are simply stated.

(i) It is clear that simple elastic unitarization is not sufficient to obtain smooth Regge behavior, even with the added effect of the FESR. Our use of the FESR does

<sup>30</sup> Since we are using  $V(s,t)$  only as the non-crossing-symmetric  $K$  matrix, we can use a form that does not have degenerate trajectories for the  $f^0$  and  $\rho$ ;  $V(s,t)$  becomes then simply a useful expression that has poles in  $\alpha_i(s)$  and asymptotic behavior governed by  $\alpha_j(t)$ . These can be different trajectories.

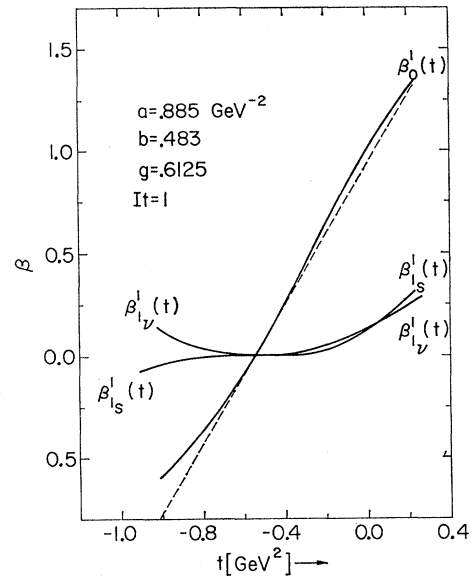


FIG. 5. Residue functions of leading and first daughter trajectories calculated from Veneziano formula for  $I_t=1$  ( $\beta_0^{I_t=0} = \frac{2}{3}\beta_0^{I_t=1}$ ). The dashed line is the straight line tangent to  $\beta_0^1(t)$  at  $t = -0.55$ . Note that a straight line provides a good approximation to  $\beta$  in this region.  $\beta_{1_s}^1(t)$  is for the expansion in  $s^{\alpha_i}$ ,  $\beta_{1_\nu}^1(t)$  for expansion  $\nu^{\alpha_i}$ .

not fix the value of the upper limit  $N$  midway between resonances as is commonly done, but rather examines the actual behavior as a function of  $N$ . One has to include some factor that causes the resonances to damp out and overlap, and we identify this factor with inelastic effects. Only then can we say that duality holds true, for the intermediate energy region of around 4–10 GeV<sup>2</sup>.

(ii) At these energies, one has to take into account "daughter" trajectories, which show up as distortions in the shape of single effective trajectories, because of interference effects. It becomes important to consider the effects of adding secondary Veneziano terms, which contribute to the lower-lying trajectories only.<sup>31</sup>

(iii) Despite the effects seen in (ii) above, the output trajectories follow the input fairly closely, except for shifts that are different for the  $I_t=0$  (the  $f^0$ ) and the  $I_t=1$  (the  $\rho$ ). Thus exchange degeneracy seems to be broken by the unitarization procedure.

Some points that should be examined if we hope to carry this study any further are essentially related to the identification of  $V^I(s,t)$  with the  $K$  matrix, and the use of a simple  $K$  matrix.

Introducing the inelastic effects as we do, by giving  $\alpha(s)$  an imaginary part, gives no inelasticity to the  $I_s=2$  amplitude, while the data of Ref. 25 do indicate the presence of appreciable inelasticity. Another defect is

<sup>31</sup> K. V. Vasavada, Phys. Rev. D 1, 88 (1970), has shown that possible secondary Veneziano terms can be added to the Lovelace model (Ref. 3) to obtain improved agreement with data out to the  $f^0$ .



TABLE I. Test of crossing-symmetry violation, within the Mandelstam triangle. The vector  $b^\sigma$  is represented columnwise with elements  $(b^\sigma)_i = a_{\sigma-l}^i$ . For the crossing-symmetric  $V(s,t)$ ,  $b_V^\sigma = \bar{b}_V^\sigma$  and  $d_V^\sigma = 1$ , so only  $b_V^\sigma$  is shown. For a unitary  $K$  matrix,  $b_K^\sigma$ ,  $\bar{b}_K^\sigma$ , and  $d_K^\sigma = b^\sigma \cdot \bar{b}^\sigma / |b^\sigma| |\bar{b}^\sigma|$  are displayed.<sup>a</sup>

$\sigma = n+l$	$b_V^\sigma$	$b_K^\sigma$	$\bar{b}_K^\sigma$	$d_K^\sigma$
0	$-2.67 \times 10^{-2}$	$-2.87 \times 10^{-2}$	$-2.87 \times 10^{-2}$	1.000
1	$-1.17 \times 10^{-2}$	$-1.24 \times 10^{-2}$	$-0.95 \times 10^{-2}$	0.984
2	$+1.17 \times 10^{-2}$	$+1.05 \times 10^{-2}$	$+1.15 \times 10^{-2}$	0.729
	$-1.82 \times 10^{-4}$	$-0.28 \times 10^{-4}$	$+3.87 \times 10^{-4}$	
	$+1.43 \times 10^{-4}$	$+6.61 \times 10^{-4}$	$+4.54 \times 10^{-4}$	
	$-1.59 \times 10^{-4}$	$-1.59 \times 10^{-4}$	$-3.37 \times 10^{-4}$	
3	$-8.12 \times 10^{-6}$	$+0.96 \times 10^{-4}$	$+1.34 \times 10^{-4}$	-0.196
	$+3.52 \times 10^{-6}$	$-2.20 \times 10^{-4}$	$+1.00 \times 10^{-4}$	
	$+1.08 \times 10^{-6}$	$+0.013 \times 10^{-4}$	$+0.09 \times 10^{-4}$	
	$+3.52 \times 10^{-6}$	$+0.035 \times 10^{-4}$	$-1.23 \times 10^{-4}$	
4	$-2.24 \times 10^{-7}$	$+1.79 \times 10^{-5}$	$+6.56 \times 10^{-4}$	0.657
	$+1.11 \times 10^{-7}$	$10.4 \times 10^{-5}$	$+5.56 \times 10^{-4}$	
	$-0.17 \times 10^{-7}$	$-0.012 \times 10^{-5}$	$+3.48 \times 10^{-4}$	
	$-0.47 \times 10^{-7}$	$-0.005 \times 10^{-5}$	$+0.36 \times 10^{-4}$	
	$-0.90 \times 10^{-7}$	$-0.009 \times 10^{-5}$	$-3.80 \times 10^{-4}$	

<sup>a</sup> Higher values of  $\sigma$  show numerical inaccuracies in the amplitudes for  $b_V^\sigma$  resulting in  $d_V^\sigma \neq 1$ . The contribution of  $b_K^\sigma$  for these values are of order  $10^{-6}$ .

that the treatment is not exactly crossing symmetric, and in fact this can be related to the lack of the above inelasticity. One method proposed to use the  $K$  matrix, but correct the lack of crossing symmetry as much as possible,<sup>3,6</sup> replaces the kinematic factor  $i\rho(s) = 2ik/\sqrt{s}$ , by a more general function. This function is chosen to have a left-hand cut, as well as the right-hand imaginary part  $2k/\sqrt{s}$ ; this is so the partial-wave amplitude generated will have left and right cuts. Lovelace's<sup>3</sup> form  $\rho_L(s)$  replaces  $\rho_0(s) = 2k/\sqrt{s}$  by

$$\rho_L(s) = \frac{2k}{\sqrt{s}} - \frac{4im_\pi^2}{\pi k \sqrt{s}} \left[ \ln \frac{\sqrt{s}}{2m_\pi} + \ln \left( 1 + \frac{2ik}{\sqrt{s}} \right) \right] \\ \equiv \rho_0(s) + \Delta\rho(s). \quad (4.1)$$

This has a limit for large  $s$  when  $\rho_0(s) \rightarrow 1$  of

$$\left( 1 + \frac{2m_\pi^2}{s} \right) - \frac{4im_\pi^2}{\pi s} \ln \frac{s}{2m_\pi^2}.$$

This form, when used in place of  $\rho_0(s)$ , gives an inelasticity to the  $I_s=2$  amplitude, governed by the  $(\ln s)/s$  term, which dies away at large  $s$ , but is significant at low and intermediate energies. Use of it corresponds to defining a different  $K$  matrix,  $K^I(s) = \rho_0(s)V^I(s)/(1-iV^I\Delta\rho)$  which now has an imaginary part, as well as a modified real part. Similarly, the  $N/D$  method, where  $N_l$  is (say) identified with  $V_l(s)$  and  $D_l$  derived by the usual relation, gives a new  $K$  matrix  $N/\text{Re}D$ . Any of these methods will damp the  $I_s=2$  amplitude somewhat, lessening the interference in (ii).

One final point in connection with the inelasticity: Although the Pomeranchukon is not included,<sup>32</sup> the belief that it is connected with the diffractive effect of all

the inelastic channels<sup>33</sup> may mean that part of the inelasticity in the data is really due to Pomeranchuk exchange in the  $t$  channel, contributing equally to each  $I_s$  channel, even at the intermediate energies. This should perhaps be subtracted from the data before comparison with the model, although exactly how to do this is not clear.

Apart from the criterion based on the inelasticity of the  $I_s=2$  amplitude, one would like to see the explicit deviation from exact crossing symmetry. To do so, it is necessary to compare the amplitude at points related by an analytic continuation in  $s$  and  $t$ . Since we use a partial-wave series to represent the amplitude, a meaningful continuation in  $t$  to a place where crossing can be checked is into the Mandelstam triangle. A continuation in  $s$  is also required; we simply replace  $k$  in  $\rho_0(s)$  by  $i\kappa$ , where  $\kappa$  is  $(4m_\pi^2 - s)^{1/2}$ . It is at this point that the singularity of  $\rho_0(s)$  at  $s=0$ , because of  $\sqrt{s}$ , becomes a nuisance. This is a reason for some of the other modifications of  $\rho_0(s)$  adopted.<sup>34,35</sup> Since our partial waves are obtained numerically, and because of the  $\sqrt{s}$  singularity, it is difficult to decide how significant the variations of the amplitude across the triangle are. Instead, we base our examination on the crossing-symmetric partial-wave expansion proposed by Balachandran and Nuyts.<sup>36</sup>

This is an expansion of the amplitude  $T(s,t)$  in terms of functions  $S_n^l(s,t)$  that are orthogonal in the two variables  $s$  and  $t$  on the triangle, and have simple crossing properties. Expanding the amplitude  $T(s,t)$ , we have

$$T(s,t) = \sum_{n,l} 2(n+l+1)(2l+1)a_n^l S_n^l(s,t),$$

where the coefficients  $a_n^l$  are obtained by the same kind of numerical integrals, as used in the above work. These coefficients obey a very simple crossing property when considered as components of a vector  $(b^\sigma)_l$ , where  $\sigma = n+l$ . It is  $\bar{b}^\sigma = b^\sigma$ , where  $(\bar{b}^\sigma)_l = \sum X_{lL}^\sigma (b^\sigma)_L$  with the  $X_{lL}^\sigma$  explicitly given in Ref. 36. Table I tabulates  $b$ ,  $\bar{b}$ , and a measure of deviation  $d = b \cdot \bar{b} / |b| |\bar{b}|$  (which is the "cosine of the angle" between the vectors), and the corresponding quantities for  $V(s,t)$  which is crossing symmetric, of course. As can be seen, not more than a few partial waves are significant in size, and they do not deviate from the corresponding values for  $V(s,t)$  by more than a few (up to 20%) percent. Use of the  $K$  matrix is clearly not crossing symmetric. The exact significance of these numbers is not clear, as the triangle is very small relative to the scale of energies we consider.

Ravenhall and Schult,<sup>34</sup> using a set of crossing-symmetric equations, find that the  $K$  matrix they ob-

<sup>33</sup> H. Harari, Phys. Rev. Letters 20, 1395 (1968).

<sup>34</sup> D. G. Ravenhall and R. L. Schult, University of Illinois report 1969 (unpublished).

<sup>35</sup> J. G. Cordes, Phys. Rev. 156, 1707 (1967).

<sup>36</sup> A. P. Balachandran and J. Nuyts, Phys. Rev. 172, 1821 (1968).

<sup>32</sup> D. Wong, Phys. Rev. 181, 1800 (1969).

tain does not differ by more than 5% from  $\rho_0(s)V(s,t)$ . Lipinski,<sup>37</sup> using crossing-symmetric sum rules identical in content to the double partial-wave analysis above, finds that Lovelace's<sup>3</sup> form violates crossing symmetry by about 8% in the  $S$  wave, and can be reduced by modifying  $\rho_L(s)$ .

The conclusion would seem to be that using  $\rho_0(s)V(s,t)$  as the  $K$  matrix is not an unreasonable first choice.

In order to consider this calculation as part of an iterative scheme that will lead to a crossing-symmetric self-consistent amplitude, a number of defects of the method must be overcome. As pointed out at the end of Sec. III, use of a partial-wave series prevents us from examining the trajectories for  $t$  very positive, and prevents us from comparing an imaginary part in the fitted  $\alpha(t)$  with that inserted in  $\alpha(s)$  in the  $K$  matrix. Then, too, we must recall that the imaginary part of  $\alpha(t)$  will correspond to the total width, as in CV, while the imaginary part of  $\alpha(s)$  is only the inelastic width.  $\text{Re}\alpha(t)$  will still be used to indicate the position of the resonances, and should be compared with  $\text{Re}\alpha(s)$ . The distortion in shape of  $\alpha(t)$  would require a form for the input more general than  $V(s,t)$ . For example we could use the form permitting logarithmic trajectories, proposed by Coon,<sup>38</sup> or we could combine a Veneziano form for the lower trajectories, with a few trajectories explicitly put in as (say)  $P_{\alpha(s)}(z_s)$ . These are problems that are encountered in any attempt to bootstrap Regge trajectories directly, if a realistic shape is required.

#### ACKNOWLEDGMENTS

The author is extremely grateful to Professor L. M. Jones and Professor D. G. Ravenhall for encouragement and many stimulating conversations throughout the course of this work. He would also like to acknowledge the continuing Post-M.Sc. bursary assistance granted by the Council for Scientific and Industrial Research of South Africa, which helped make this study possible.

#### APPENDIX: $\pi$ - $\pi$ VENEZIANO MODEL AND DAUGHTER TRAJECTORIES

The basic  $\pi$ - $\pi$  Veneziano function,<sup>10,39</sup>

$$F(s,t) = \frac{\Gamma(1-\alpha(s))\Gamma(1-\alpha(t))}{\Gamma(1-\alpha(s)-\alpha(t))}, \quad (\text{A1})$$

has  $s$  and  $t$  poles (resonances) lying on the degenerate  $\rho$ - $f^0$  trajectories  $\alpha(s)$ ,  $\alpha(t)$  at  $\alpha=n$ ,  $n=1, 2, \dots$ . The

<sup>37</sup> H. M. Lipinski, University of Wisconsin Report No. C00-264, 1969 (unpublished).

<sup>38</sup> D. D. Coon, Phys. Letters **29B**, 669 (1969). The objections to this form, on the grounds of crossing symmetry and Regge behavior, raised by F. Capra, *ibid.* **30B**, 53 (1969), do not apply if the form is used as a  $K$  matrix, which is not crossing symmetric. See Ref. 30.

<sup>39</sup> K. Kang, Nuovo Cimento Letters **3**, 576 (1970). J. Yellin, Phys. Rev. **182**, 1482 (1969).

$s$ -channel isospin-2 amplitude  $V^{I=2}(s,t,u)$  is equal to  $gF(u,t)$ .

We display the  $s$ -channel poles and polynomial residues by using an expansion that converges in the  $s$ -channel physical region,

$$F(s,t) = \sum_{n=1}^{\infty} \frac{\Gamma(n+\alpha(t))}{\Gamma(\alpha(t))\Gamma(n)} \frac{1}{n-\alpha(s)} \\ = \sum_{n=1}^{\infty} \frac{R_n(t)}{s_n-s}, \quad R_n(t) = \frac{[\alpha(t)]_n}{a(n-1)!}, \quad (\text{A2})$$

with  $s_n$  defined by  $\alpha(s_n)=n$ , and  $[\alpha(t)]_n \equiv [n-1+\alpha(t)] \times [n-2+\alpha(t)] \cdots \alpha(t)$ .

The Regge asymptotic limit for fixed  $t$  and  $s \rightarrow \infty$  is easily seen using the Stirling approximation for the gamma function which gives the leading behavior,

$$\Gamma(y+b)/\Gamma(y) \rightarrow y^b \quad \text{as } |y| \rightarrow \infty,$$

dominated by the  $t$ -channel parent trajectory. By using further terms in the expansion of the ratio of two gamma functions, we can find lower powers of  $s$  [or of  $\nu = \frac{1}{2}(s-u)$  for symmetry] corresponding to the effect of daughters,<sup>40</sup>

$$\frac{\Gamma(y+c)}{\Gamma(y+f)} = \sum_{k=0}^N y^{c-f-k} A_k^c(c-f) + O(y^{c-f-N-1}), \\ \text{Re}y > 0 \quad (\text{A3})$$

with the first terms<sup>41</sup>

$$A_0 = 1, \\ A_1 = \frac{1}{2}(c-f)(c+f-1), \\ A_2 = (1/24)(c-f)(c-f-1) \\ \times [3(c+f-1)^2 - c + f - 1]. \quad (\text{A4})$$

The high-energy behavior is controlled by Regge poles corresponding to resonances in the  $t$  channel, so we look at the  $t$ -channel isospin amplitudes. Lack of  $I_t=2$  resonances requires  $V_t^2(s,t,u) = gF(s,u)$  to vanish (contribute to the background) and it will vanish exponentially with  $s$  if  $I(s)/\ln s \rightarrow \infty$ , where  $I(s)$  is the imaginary part of  $\alpha(s)$  that we add to display the Regge limit by displacing the resonance poles,  $1/\sin\pi\alpha$ , from the real axis. To obtain the correct signature factor, we also require  $I(s)/s \rightarrow 0$ . If  $I(s)$  is small or zero,  $F(s,u)$  will appear to go as  $s^{y'}$ , with  $y'$  lower than the leading trajectory,  $y=\alpha(t)$ , by amount  $d=3b+a\Sigma-1 \approx 0.57$  (where  $\Sigma=4m_\pi^2$ ). Even with a rising  $I(s)$ , this effect may be observed for small values of  $s$ .

<sup>40</sup> D. I. Fivel and P. K. Mitter, Phys. Rev. **183**, 1240 (1969); F. Drago and S. Matsuda, *ibid.* **181**, 2095 (1969).

<sup>41</sup> N. N. Khuri, Phys. Rev. **185**, 1876 (1969).

Performing the expansion, we obtain the Regge limits  $y = a\nu$ :

$$V_t^0(s, t, y) \rightarrow \sum_{L=0}^N -\beta_L^0(t) \frac{+1 + e^{-i\pi\alpha_L(t)}}{\sin\pi\alpha_L(t)} y^{\alpha_L(t)},$$

$$V_t^1(s, t, u) \rightarrow \sum_{L=0} -\beta_L^1(t) \frac{-1 + e^{-i\pi\alpha_L(t)}}{\sin\pi\alpha_L(t)} y^{\alpha_L(t)}, \quad (\text{A5})$$

$$V_t^2(s, t, u) \rightarrow 0,$$

with the daughter trajectories  $\alpha_L(t) \equiv \alpha(t) - L$ .

The leading residues are

$$\begin{aligned} \beta_0^0(t) &= \frac{3}{2}\pi g / \Gamma(\alpha(t)), \\ \beta_0^1(t) &= \pi g / \Gamma(\alpha(t)), \end{aligned} \quad (\text{A6})$$

and  $y$  is either  $as$  or  $a\nu$ . The residues after the first depend on whether  $y = as$  or  $a\nu$ , as could be expected. In fact, we only get the correct signature factor if we use  $y = a\nu$ , since then the coefficients of the expansion of  $F(s, t)$  and  $F(u, t)$  are the same. If we expand in  $as$ , we will get the signature by forcing symmetry in the FESR. This is possible because in the FESR we use only  $\text{Im}T^I(s)$  and only  $F(s, t)$  contributes to the right-hand cut.

Recalling that  $u = \Sigma - t - s = \Sigma(t) - \nu$  and  $s = \Sigma(t) + \nu$  with  $\Sigma(t) = \frac{1}{2}(\Sigma - t)$ , we find for  $F(s, t)$

$y = as$ :

$$\begin{aligned} c &= b + \alpha(t), & x &= c - f = \alpha(t), \\ f &= b, & w &\equiv c + f - 1 = 3b + at - 1; \end{aligned} \quad (\text{A7})$$

$y = a\nu$ :

$$\begin{aligned} c &= b + \alpha(t) + a\Sigma(t), & x &= \alpha(t), \\ f &= b + a\Sigma(t), & w &\equiv 3b + a\Sigma - 1; \end{aligned}$$

and for  $F(u, t)$

$y = as$ :

$$\begin{aligned} c &= 1 - b - 2a\Sigma(t), & x &= \alpha(t), \\ f &= 1 - b - 2a\Sigma(t) - \alpha(t), & w &\equiv 1 - 3b - 2a\Sigma + at; \end{aligned} \quad (\text{A8})$$

$$\begin{aligned} c &= 1 - b - a\Sigma(t), & x &= \alpha(t), \\ f &= 1 - b - a\Sigma(t) - \alpha(t), & w &\equiv 1 - 3b - a\Sigma. \end{aligned}$$

For the  $a\nu$  case it is important to notice that  $w$  for  $F(s, t)$  is  $-w$  for  $F(u, t)$ . This gives the correct signature then, since the expansion of  $F(s, t)$  is in powers of  $a\nu$  and should be in powers of  $(-a\nu) = e^{-i\pi}(a\nu)$ . This ensures that we have  $(\tau + e^{-i\pi\alpha_k(t)})$  as the signature factor in the expressions [recall that  $\sin\pi\alpha_0 = (-1)^k \sin\pi\alpha_k$ ].

With the first three terms explicit, in the  $a\nu$  case we have

$$\begin{aligned} F(s, t) &= f(-a\nu, t) = \frac{\pi(-a\nu)^{\alpha(t)}}{\Gamma(\alpha(t))} \\ &\times \left( 1 + \frac{\alpha(t)}{2(-a\nu)} [1 - 3b - a\Sigma] + \frac{\alpha(t)(\alpha(t) - 1)}{24(-a\nu)^2} \right. \\ &\quad \left. \times [3(1 - 3b - a\Sigma)^2 - \alpha(t) - 1] \dots \right), \end{aligned} \quad (\text{A9})$$

$$F(u, t) = f(a\nu, t),$$

so that we get

$$\begin{aligned} \beta_1^I &= -\beta_0^I(t) [1 - 3b - a\Sigma] \alpha(t) / 2, \\ \beta_2^I &= \beta_0^I(t) [3(1 - 3b - a\Sigma)^2 - \alpha(t) - 1] \\ &\quad \times \alpha(t) [\alpha(t) - 1] / 24. \end{aligned} \quad (\text{A10})$$

[The  $(-1)$  in  $\beta_1^I$  is from replacing  $\sin\pi\alpha_0$  by  $-\sin\pi\alpha_1$ .] For the  $as$  case, we use the residues arising from  $F(s, t)$  which are the same as above, except for  $a\Sigma$  being replaced by  $at$ .

For computational purposes, it is easier to include the scale factor  $a$  in the residues, and expand only in powers of  $\nu$  or  $s$ . This is simply an exponential factor  $(a)^{\alpha_k(t)}$ , inserted into  $\beta_k$ :  $\tilde{\beta}_k^I(t) = \beta_k^I(t) a^{\alpha_k(t)}$ , used instead of  $\beta_k^I(t)$ .

With the Lovelace<sup>3</sup> parameters  $a = 0.885$  and  $b = 0.483$ , we find  $(1 - 3b - a\Sigma) \cong -0.52$ . Figure 5 displays  $\beta_0^1(t)$  and  $\beta_1^1(t)$  for the  $s$  and  $\nu$  cases.